

Pyrrolinone-Based HIV Protease Inhibitors. Design, Synthesis, and Antiviral Activity: Evidence for Improved Transport

Amos B. Smith, III,^{*,†} Ralph Hirschmann,^{*,†} Alexander Pasternak,[†] Mark C. Guzman,[†] Akihisa Yokoyama,[†] Paul A. Sprengeler,[†] Paul L. Darke,[‡] Emilio A. Emini,[‡] and William A. Schleif[‡]

Contribution from the Department of Chemistry, University of Pennsylvania, Philadelphia, Pennsylvania 19104, and Departments of Molecular Biology and Virus and Cell Biology, Merck Research Laboratories, West Point, Pennsylvania 19486

Received April 28, 1995[®]

Abstract: Pyrrolinone-based peptidomimetics, the first mimics of β -strands, are potent inhibitors of HIV-1 protease. Importantly, the bis(pyrrolinones) described herein proved to be more active in cellular antiviral assays compared with an analogous peptide-derived inhibitor even though they are less effective in inhibiting the isolated protease. These results suggest that pyrrolinone inhibitors offer better transport properties than the corresponding peptide-based peptidomimetics; we attribute this effect to decreased solvation of the mimetics. Structure–activity relationships for the pyrrolinones correlate well with those reported for related peptides, consistent with similar modes of binding.

In recent years intensive efforts have been directed toward the design, synthesis, and utilization of non-peptide peptidomimetics.¹ These investigations have been prompted, in part, by the generally unfavorable pharmacokinetic properties of peptides.^{1,2} In addition, peptidomimetics have been exploited as probes of the bioactive conformations of endogenous peptide ligands.^{1,3}

[†] University of Pennsylvania.

[‡] Merck Research Laboratories.

[®] Abstract published in *Advance ACS Abstracts*, November 1, 1995.

(1) For reviews, see: (a) Hirschmann, R. *Angew. Chem., Int. Ed. Engl.* **1991**, *30*, 1278. (b) Schiller, P. W. In *Medicinal Chemistry for the 21st Century*; Wermuth, C. G., Koga, N., Konig, H., Metcalf, B. W., Eds.; Blackwell Scientific Publications: Oxford, U.K., 1992; Chapter 15. (c) Giannis, A.; Kolter, T. *Angew. Chem., Int. Ed. Engl.* **1993**, *32*, 1244. (d) Olson, G. L.; Bolin, D. R.; Bonner, M. P.; Bos, M.; Cook, C. M.; Fry, D. F.; Graves, B. J.; Hatada, M.; Hill, D. E.; Kahn, M.; Madison, V. S.; Rusiecki, V. K.; Sarabu, R.; Sepinwall, J.; Vincent, G. P.; Voss, M. E. *J. Med. Chem.* **1993**, *36*, 3039. (e) Liskamp, R. M. J. *Recl. Trav. Chim. Pays-Bas* **1994**, *113*, 1. (f) Gante, J. *Angew. Chem., Int. Ed. Engl.* **1994**, *33*, 1699. See also: (g) Nicolaou, K. C.; Salvino, J. M.; Raynor, K.; Pietranico, S.; Reisine, T.; Freidinger, R. M.; Hirschmann, R. In *Peptides—Chemistry, Structure and Biology: Proceedings of the 11th American Peptide Symposium*; Rivier, J. E., Marshall, G. R., Eds.; ESCOM: Leiden, The Netherlands, 1990; pp 881–884. (h) Hirschmann, R.; Nicolaou, K. C.; Pietranico, S.; Salvino, J.; Leahy, E. M.; Sprengeler, P. A.; Furst, G.; Smith, A. B., III; Strader, C. D.; Cascieri, M. A.; Candelore, M. R.; Donaldson, C.; Vale, W.; Maechler, L. *J. Am. Chem. Soc.* **1992**, *114*, 9217. (i) Hirschmann, R.; Sprengeler, P. A.; Kawasaki, T.; Leahy, J. W.; Shakespeare, W. C.; Smith, A. B., III. *J. Am. Chem. Soc.* **1992**, *114*, 9699. (j) Hirschmann, R.; Sprengeler, P. A.; Kawasaki, T.; Leahy, J. W.; Shakespeare, W. C.; Smith, A. B., III. *Tetrahedron* **1993**, *49*, 3665. (k) Hirschmann, R.; Nicolaou, K. C.; Pietranico, S.; Leahy, E. M.; Salvino, J.; Arison, B.; Cichy, M. A.; Spoors, P. G.; Shakespeare, W. C.; Sprengeler, P. A.; Hamely, P.; Smith, A. B., III; Reisine, T.; Raynor, K.; Maechler, L.; Donaldson, C.; Vale, W.; Freidinger, R. M.; Cascieri, M. R.; Strader, C. D. *J. Am. Chem. Soc.* **1993**, *115*, 12550. (l) Smith, A. B., III; Keenan, T. P.; Holcomb, R. C.; Sprengeler, P. A.; Guzman, M. C.; Wood, J. L.; Carroll, P. J.; Hirschmann, R. *J. Am. Chem. Soc.* **1992**, *114*, 10672. (m) Smith, A. B., III; Hirschmann, R.; Pasternak, A.; Akaishi, R.; Guzman, M. C.; Jones, D. R.; Keenan, T. P.; Sprengeler, P. A.; Darke, P. L.; Emini, E. A.; Holloway, M. K.; Schleif, W. A. *J. Med. Chem.* **1994**, *37*, 215. (n) Smith, A. B., III; Guzman, M. C.; Sprengeler, P. A.; Keenan, T. P.; Holcomb, R. C.; Wood, J. L.; Carroll, P. J.; Hirschmann, R. *J. Am. Chem. Soc.* **1994**, *116*, 9947. (o) Smith, A. B., III; Akaishi, R.; Jones, D. R.; Keenan, T. P.; Guzman, M. C.; Holcomb, R. C.; Sprengeler, P. A.; Wood, J. L.; Hirschmann, R.; Holloway, M. K. *Peptide Sci.* **1995**, *37*, 29. (p) Hirschmann, R.; Smith, A. B., III; Sprengeler, P. A. In *New Perspectives in Drug Design*; Dean, P. M., Jolles, G., Newton, C. G., Eds.; Academic: London, 1995; Vol. 35, pp 4271–4274.

(2) (a) Moffat, A. S. *Science* **1993**, *260*, 910. (b) Wallace, B. M.; Lasker, J. S. *Science* **1993**, *260*, 912.

The prevalent strategy for peptidomimetic design involves the enforced emulation of specific motifs of peptide secondary structure.¹ This approach reflects the accepted view that biologically active peptides adopt discrete conformations upon binding, even though many energetically similar conformations are accessible. Peptidomimetics based upon the β -strand motif, which previously attracted relatively little attention, have gained considerable importance with the discovery that peptidyl substrates and inhibitors bind to diverse proteolytic enzymes as β -strands.^{3,1a} Notably, X-ray studies revealed β -strand bound conformations for inhibitors of the HIV protease, an aspartic acid protease required for processing of the viral polyprotein precursor (*vide infra*).⁴

Recently we reported the design and synthesis of β -strand mimics in which a novel, linked 3,5,5-pyrrolin-4-one scaffolding entirely replaced the native peptide backbone (e.g., **1** \rightarrow **2**, Figure 1).^{11a} Tetrapeptide **1**, a fragment of equine angiotensinogen, exists in the solid state as a parallel β -pleated sheet; we have demonstrated that the analogous urethane-protected tris(pyrrolinone) **2** crystallizes as an antiparallel β -sheet. The corresponding free amine, like **1**, crystallizes as a parallel β -pleated sheet. The side-chain trajectories and pyrrolinone carbonyl orientations of **2** closely correspond with those of tetrapeptide **1**. Importantly, the formation of β -pleated sheets in the solid state implied that the nitrogens, although displaced from their usual positions on the backbone, were nonetheless capable of

(3) (a) James, M. N. G.; Sielecki, A.; Salituro, F.; Rich, D. H.; Hofmann, T. *Proc. Natl. Acad. Sci. U.S.A.* **1982**, *79*, 6137. (b) Foundling, S. I.; Cooper, J.; Watson, F. E.; Cleasby, A.; Pearl, L. H.; Sibanda, B. L.; Hemmings, A.; Wood, S. P.; Blundell, T. L.; Valler, M. J.; Norey, C. G.; Kay, J.; Boger, J.; Dunn, B. M.; Leckie, B. J.; Jones, D. M.; Atrash, B.; Hallett, A.; Szelke, M. *Nature* **1987**, *327*, 349. (c) Suguna, K.; Padlan, E. A.; Smith, C. W.; Carlson, W. D.; Davies, D. R. *Proc. Natl. Acad. Sci. U.S.A.* **1987**, *84*, 7009. (d) Sawyer, T. K.; Pals, D. T.; Mao, B.; Maggiora, L. L.; Staples, D. J.; deVaux, A. E.; Schostarez, H. J.; Kinner, J. H.; Smith, C. W. *Tetrahedron* **1988**, *44*, 661. (e) Rich, D. H. In *Comprehensive Medicinal Chemistry*; Sammes, P. G., Taylor, J. B., Eds.; Pergamon: New York, 1990; Vol. 4, p 391.

(4) (a) Farmerie, W. G.; Loeb, D. D.; Cassavant, N. C.; Hutchinson, C. A., III; Edgell, M. H.; Swannstrom, R. *Science* **1987**, *236*, 305. (b) Mervis, R. J.; Ahmad, N.; Lillehoj, E. P.; Raum, M. G.; Salazar, F. H. R.; Chan, H. W.; Venkatesan, S. *J. Virol.* **1988**, *62*, 3993. (c) Kräusslich, H.-G.; Wimmer, E. *Annu. Rev. Biochem.* **1988**, *57*, 701. (d) Kohl, N. E.; Emini, E. A.; Schleif, W. A.; Davis, L. J.; Heimbach, J. C.; Dixon, R. A. F.; Scolnick, E. M.; Sigal, I. S. *Proc. Natl. Acad. Sci. U.S.A.* **1988**, *85*, 4686.

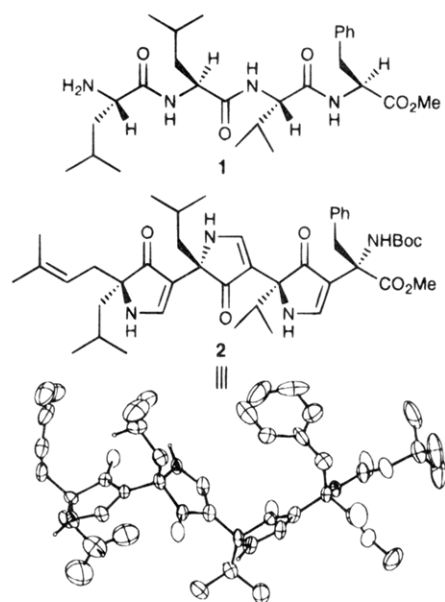


Figure 1. Tetrapeptide equine angiotensinogen fragment **1**; structure and solid-state β -strand conformation of tris(pyrrolinone) peptidomimetic **2**.

forming interstrand hydrogen bonds. These features were considered essential for effective inhibition of aspartic acid proteases, as recognition and binding require both specific side-chain and backbone hydrogen bond interactions.^{1a,5} These pyrrolinones thus represent the first peptidomimetics of β -pleated sheets.

Via this strategy we subsequently generated biologically active inhibitors of the aspartic acid proteases renin and HIV-1 protease.^{1m} A full account of the renin work has already appeared.^{1o} Herein we describe in detail the design, synthesis, and antiviral activity of a series of novel pyrrolinone-based HIV-1 protease inhibitors.

Design of an HIV-1 Protease Inhibitor Incorporating the Pyrrolinone Scaffold. The X-ray structures of diverse inhibitors bound to HIV-1 protease revealed that many binding interactions are conserved.⁶ Moreover, substrates of this enzyme contain a variety of amino acid sequences on either side of the scissile bond, suggesting that sequence requirements may be less important than *substrate conformation* for recognition.^{6a,7} Inhibitors bind in the active site in extended β -strand conformations with the side chains inserted into adjacent lipophilic pockets of the enzyme, as exemplified by the X-ray-derived representations of the bound inhibitors MVT-101 (Figure 2) and JG-365 (not shown).⁸ The solid-state conformation of tris(pyrrolinone) **2** (Figure 1) strikingly mimics the pleated backbone conformations and antiperiplanar side-chain trajectories observed for both MVT-101 and JG-365. Accordingly, preorganization of pyrrolinone-based inhibitor of HIV-1 protease

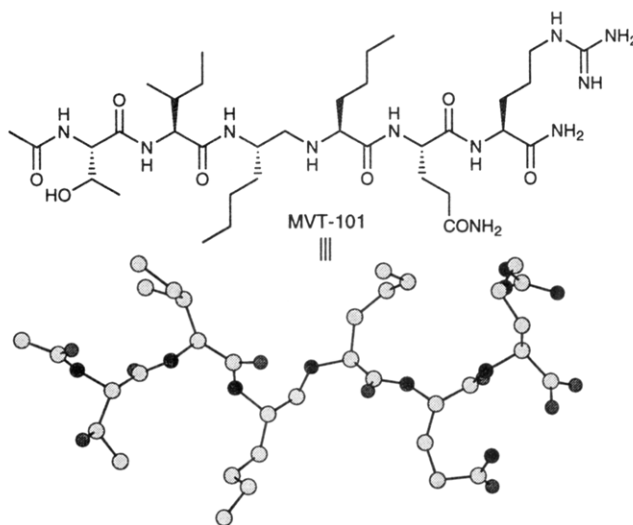


Figure 2. Enzyme-bound conformation of HIV protease inhibitor MVT-101.

was expected to promote recognition and binding, in accord with the pioneering studies of host/guest complexation by Cram et al.⁹

Other elements of our design derived from the structure of L-682,679 (Figure 3), a potent inhibitor of the HIV protease ($IC_{50} = 0.4$ nM, $CIC_{95} = 6$ μ M).¹⁰ The P_1 - P_3 tripeptide sequence of L-682,679 was replaced by a bis(pyrrolinone) bearing the three requisite side chains. The P_1 Phe,¹¹ the hydroxyethyl transition-state mimetic, and the N- and C-terminal endcaps were also adopted, leading to **3** as our prototypical target.

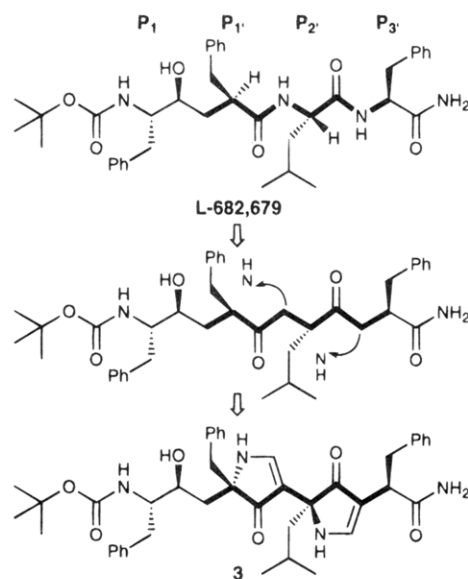


Figure 3. Merck inhibitor L-682,679 as the model for a prototypical pyrrolinone-based inhibitor **3**. Pyrrolinone motif is generated by NH displacement from peptide backbone.

Molecular Modeling. We generated an initial conformation of **3**, analogous to the X-ray crystal structures of peptid

(5) Rudinger, J. In *Drug Design*; Ariens, E. J., Ed.; Academic: New York, 1971; Vol. 2, p 319.

(6) (a) Huff, J. R. *J. Med. Chem.* **1991**, *34*, 2305. (b) Swain, A. L.; Miller, M. M.; Green, J.; Rich, D. H.; Schneider, J.; Kent, S. B. H.; Wlodawer, A. *Proc. Natl. Acad. Sci. U.S.A.* **1990**, *87*, 8805.

(7) Newlander, K. A.; Callahan, J. F.; Moore, M. L.; Tomaszek, T. A., Jr.; Huffman, W. F. *J. Med. Chem.* **1993**, *36*, 2321.

(8) Miller, M.; Schneider, J.; Sathyanarayana, B. K.; Toth, M. V.; Marshall, G. R.; Clawson, L.; Selk, L.; Kent, S. B. H.; Wlodawer, A. *Science* **1989**, *246*, 1149.

(9) Cram, D. J. *Science* **1988**, *240*, 760. Cram, D. J.; Lein, G. M. *J. Am. Chem. Soc.* **1985**, *107*, 3657. For another application of this concept to the design of HIV-1 protease inhibitors, see: Lam, P. Y. S.; Jadhav, P. K.; Eyermann, C. J.; Hodge, C. N.; Ru, Y.; Bacheler, L. T.; Meek, J. L.; Otto, M. J.; Rayner, M. M.; Wong, Y. N.; Chang, C.-H.; Weber, P. C.; Jackson, D. A.; Sharpe, T. R.; Erickson-Viitanen, S. *Science* **1994**, *263*, 380.

(10) (a) Huff, J. R.; Anderson, P. S.; Britcher, S. F.; Darke, P.; deSolms, S. J.; Dixon, R. A. F.; Emini, E.; Hoffman, J. M.; Lyle, T. A.; Randall, W. C.; Rooney, C. S.; Sigal, I. S.; Sweet, C. S.; Thompson, W. J.; Vacca, J. P.; Young, S. D. *J. Cell Biochem. Suppl.* **1990**, *14C*, 222. (b) deSolms, S. J.; Giuliani, E. A.; Guare, J. P.; Vacca, J. P.; Sanders, W. M.; Graham, S. L.; Wiggins, J. M.; Darke, P. L.; Sigal, I. S.; Zugay, J. A.; Emini, E. A.; Schleif, W. A.; Quintero, J. C.; Anderson, P. S.; Huff, J. R. *J. Med. Chem.* **1991**, *34*, 2852.

(11) Schechter, I.; Berger, A. *Biochem. Biophys. Res. Commun.* **1967**, *27*, 157.

inhibitors MVT-101 (Figure 2) and JG-365 bound to the protease.¹² This exercise entailed substitution of two pyrrolinone units in their lowest-energy linear conformations for the P₁–P₂' and P₂'–P₃' amide bonds, as well as incorporation of appropriate side chains and end capping. Energy minimization with the MM2 force field¹³ then furnished a local minimum (Figure 4a), which was similar to the initial conformation; importantly, the minimized structure also closely resembled the *global* minima obtained in more extensive computational analysis of related bis(pyrrolinones). Least-squares comparisons with the solid state conformation of enzyme-bound MVT-101 (Figure 4b) indicated that **3** can easily adopt the conformation required for binding. Docking into the HIV-1 protease active site¹⁴ revealed no unfavorable steric interactions. Moreover, the docking study suggested that the pyrrolinone carbonyls of **3** should hydrogen bond with similar geometries to the same enzyme NH groups as the amide carbonyls of cocrystallized peptidic inhibitor MVT-101. The pyrrolinone NH moieties were likewise predicted to H-bond with the same enzyme groups as the backbone amide NH's of MVT-101, albeit necessarily with different geometries.

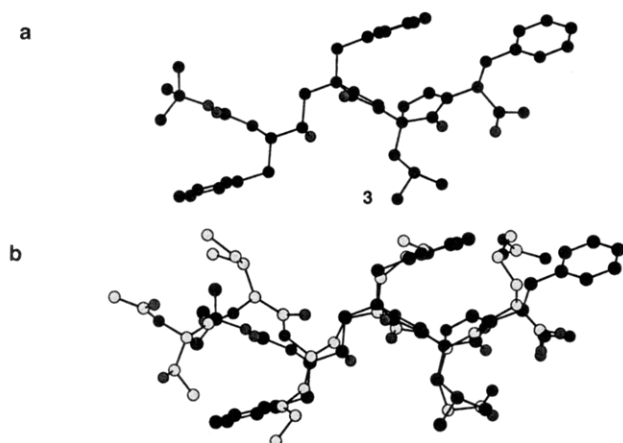


Figure 4. (a) MM2-minimized extended conformation of proposed bis(pyrrolinone) inhibitor **3**. (b) Least-squares comparisons of **3** (black) with inhibitor MVT-101 (gray).

Synthesis of Bis(pyrrolinone) Inhibitor 3. As outlined retrosynthetically in Figure 5, we envisioned a highly convergent approach to **3** via precursors of comparable complexity (i.e., **4** and **5**). We elected to prepare pyrrolinone **5** from the α,α -disubstituted amino ester **6** and aldehyde **7**, exploiting our well-established cyclization protocol.¹⁵ The aldehyde in turn would derive from Evans asymmetric alkylation chemistry.¹⁶ We planned to construct **4** via alkylation of the enolate of oxazolidinone **9** with iodide **8**.

In the event, the synthesis of **5** proceeded smoothly (Scheme 1). Acylation of the Evans oxazolidinone (–)-**10** with hydrocinnamoyl chloride and alkylation with prenyl bromide furnished

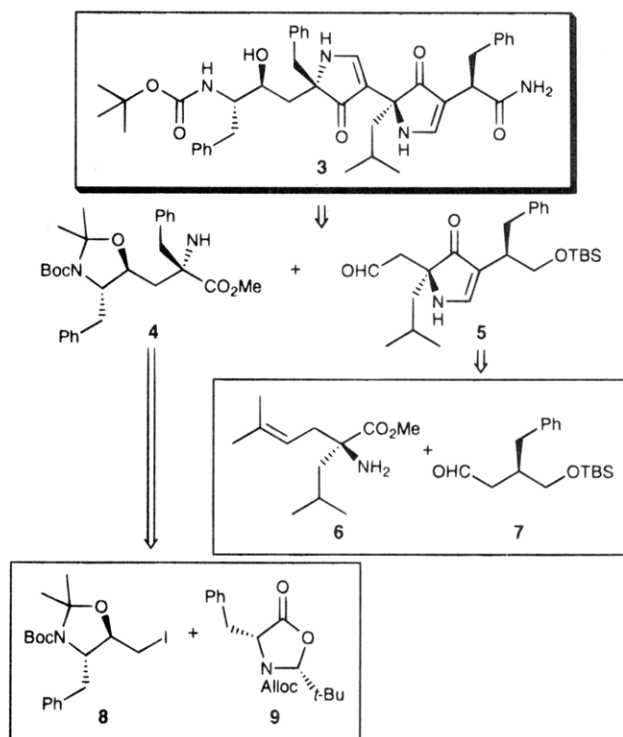
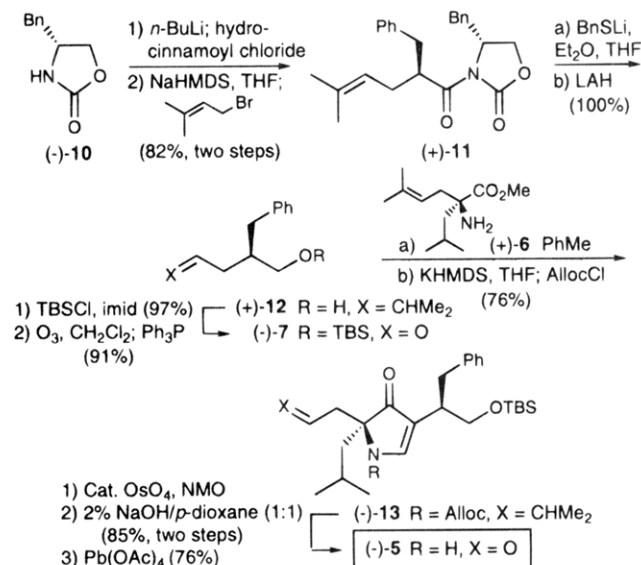


Figure 5. Retrosynthetic analysis of target inhibitor **3**.

(+)-**11** with good diastereoselectivity (82% yield for two steps). Following removal of the chiral auxiliary with benzyl thiolate,¹⁷ LAH reduction of the intermediate thio ester quantitatively afforded primary alcohol (+)-**12**. Hydroxyl protection as the TBS ether (97% yield) and reductive ozonolysis (91%) then gave aldehyde (+)-**7**.

Scheme 1



Pyrrolinone cyclization was effected in conjunction with *in situ* protection of the product amine. Condensation of **7** with the known α,α -disubstituted amino ester (+)-**6**,¹⁵ followed by KHMDS deprotonation of the resultant imine, and N-acylation with allyl chloroformate furnished mono(pyrrolinone) (–)-**13** in 76% yield. Oxidative cleavage of the prenyl side chain of **13**, required for elaboration of the second pyrrolinone, was then undertaken via our usual two-step procedure. Dihydroxylation

(12) MacroModel, ver. 3.1X: Still, W. C.; Mohamadi, F.; Richards, N. G. J.; Guida, W. C.; Lipton, M.; Liskamp, R.; Chang, G.; Hendrickson, T.; DeGust, F.; Hasel, W. Department of Chemistry, Columbia University, New York, NY 10027.

(13) The 1987 version of the MM2 force field was used: Bowen, J. P.; Pathiaseril, A.; Profeta, S., Jr.; Allinger, N. L. *J. Org. Chem.* **1987**, *52*, 5162. See also: Allinger, N. L. *J. Am. Chem. Soc.* **1977**, *99*, 8127.

(14) X-ray coordinates for complexes of HIV-1 protease with inhibitors MVT-101 and JG-365 were kindly provided by Dr. A. Wlodawer (NIH, Bethesda, MD), see refs 6b and 8. A stereodiagram of **3** docked into the MVT-101/HIV-1 protease X-ray structure active site is included in the supporting information.

(15) Smith, A. B., III; Holcomb, R. C.; Guzman, M. C.; Keenan, T. P.; Sprengler, P. A.; Hirschmann, R. *Tetrahedron Lett.* **1993**, *34*, 63.

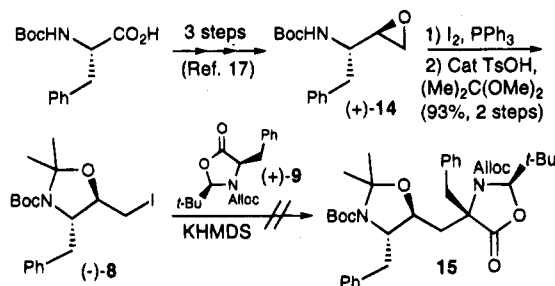
(16) Evans, D. A.; Ennis, M. D.; Mathre, D. J. *J. Am. Chem. Soc.* **1982**, *104*, 1737.

(17) Damon, R. E.; Coppola, G. M. *Tetrahedron Lett.* **1990**, *31*, 2849.

with a catalytic amount of OsO₄ and excess NMO proceeded with concomitant oxidation of the Alloc protecting group; the latter moiety proved to be necessary to prevent oxidation of the pyrrolinone double bond. We note here that competing oxidation of pyrrolinone olefins with OsO₄/NMO occurs only when the allylic carbon is tertiary. Normally this position is quaternary, as our standard mono(pyrrolinone) units derive from two α,α -disubstituted amino esters; in these latter cases the vinylogous amide double bond does not react. Following removal of the hydroxylated Alloc group with a mixture of 2% aqueous NaOH and *p*-dioxane (1:1) (85% yield from **13**), oxidative diol cleavage with Pb(OAc)₄ provided the corresponding aldehyde, mono(pyrrolinone) building block (–)-**5**, in 76% yield.

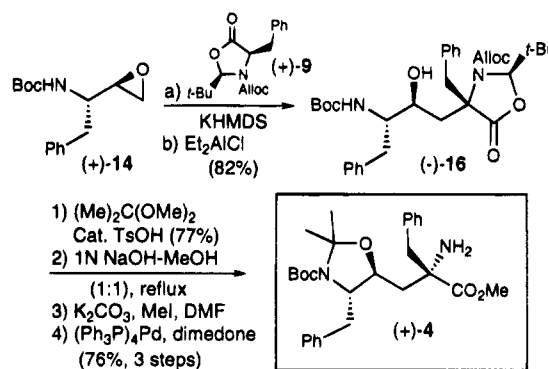
The synthesis of amine subunit **4** began with the known epoxide (+)-**14**, prepared from Boc-Phe.¹⁸ Pursuant to our initial strategy, the epoxide was converted to protected iodohydrin (–)-**8** (Scheme 2). Diastereoselective alkylation of oxazolidinone (+)-**9**, derived from D-Phe, with iodide **8** via the Karady/Seebach protocol¹⁹ was then intended to furnish the complete backbone of **4**. Unfortunately, the coupling of **9** with **8** failed under a variety of experimental conditions; this result was not entirely unexpected, as Karady/Seebach oxazolidinone alkylations normally require highly reactive electrophiles such as benzyl, allyl, or methyl halides.²⁰ In an effort to circumvent this limitation, we next explored the direct alkylation of the enolate of **9** with epoxide **14**, a process apparently without precedent.²¹ The desired ring-opened adduct was readily

Scheme 2



obtained under the influence of Lewis acids. Initial experiments with BF₃·OEt₂ afforded alcohol **16** in modest yield (28–33%) as a 7:1 mixture of epimers. Ultimately we discovered that addition of diethylaluminum chloride to a mixture of the enolate and epoxide at –78 °C gave alcohol (–)-**16** in 82% yield with >97% diastereoselectivity (Scheme 3).²² Protection of the carbamate nitrogen and hydroxyl of **16** as an acetonide (77%

Scheme 3



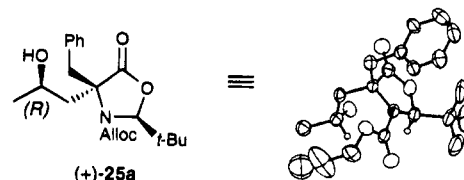
yield), cleavage of the oxazolidinone ring, methyl ester formation, and Alloc removal (76% for three steps) then furnished amino ester (+)-**4**, suitable for union with **5**.

Alkylation of Oxazolidinone Aluminum Enolates with Epoxides: Scope and Limitations. Recognizing that the alkylation of oxazolidinone enolates with epoxides, if general, would constitute a valuable approach to homoserine analogs, we completed a parallel investigation of this methodology. The protocol developed enables the alkylation of oxazolidinones derived from a variety of amino acids with ethylene oxide and monosubstituted epoxides (Table 1).²² Diastereoselectivities generally exceeded 95%.

Following hydroxyl protection, the alkylated oxazolidinones readily furnish the corresponding amino esters via established chemistry.^{15,19} In the simple systems the alcohol was masked as a MEM ether, as illustrated in Scheme 4. Hydrolysis (1 N NaOH/MeOH, 1:1), esterification of the resultant carboxylic acid (K₂CO₃, DMF; MeI), and removal of the Alloc protecting group [Pd(PPh₃)₄ catalyst, dimedone] then afforded the target homoserine derivative (e.g., **26**).

Elaboration of **3, the Target Bis(pyrrolinone) Inhibitor.** The synthesis of **3** proceeded uneventfully with the union of **5** and **4**, executed via our now-standard protocol.¹⁵ In situ Alloc protection of both pyrrolinones gave (+)-**27**, a key intermediate containing all of the backbone carbons and stereocenters of the target compound, in 76% yield (Scheme 5). Treatment of **27** with Jones reagent in MeCN at –39 °C led to desilylation and oxidation of the resultant alcohol to the corresponding carboxylic acid (75% yield). The N-terminal Boc moiety remained intact under these conditions. We also noted that deprotection of the pyrrolinone nitrogens prior to oxidation resulted in lower yields of the carboxylic acid. Subsequent Pd(0)-catalyzed removal of the Alloc groups followed by primary amide formation via a mixed anhydride furnished (–)-**28** (85% yield, two steps). Finally, after removal of the acetonide and Boc moieties with methanolic HCl, the N-terminal Boc endcap could be reinstalled to give (–)-**3** in 64% yield. Selective alcoholysis of the

(23) An X-ray crystal structure verified the relative stereochemistry of the major isomer **25a**.



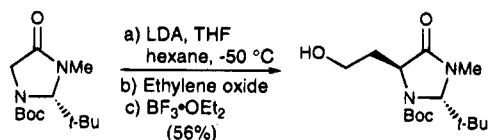
(24) (a) Heimbach, J. C.; Garsky, V. M.; Michelson, S. R.; Dixon, R. A. F.; Sigal, I. S.; Darke, P. L. *Biochem. Biophys. Res. Commun.* **1989**, *164*, 955. (b) Thompson, W. J.; Fitzgerald, P. M. D.; Holloway, M. K.; Emini, E. A.; Darke, P. L.; McKeever, B. M.; Schleif, W. A.; Quintero, J. C.; Zugay, J. A.; Tucker, T. J.; Schwering, J. E.; Homnick, C. F.; Nunberg, J.; Springer, J. P.; Huff, J. R. *J. Med. Chem.* **1992**, *35*, 1685.

(18) Thompson, W. J.; Fitzgerald, P. M. D.; Holloway, M. K.; Emini, E. A.; Darke, P. L.; McKeever, B. M.; Schleif, W. A.; Quintero, J. C.; Zugay, J. A.; Tucker, T. J.; Schwering, J. E.; Homnick, C. F.; Nunberg, J.; Springer, J. P.; Huff, J. R. *J. Med. Chem.* **1992**, *35*, 1685.

(19) (a) Karady, S.; Amato, J. S.; Weinstock, L. M. *Tetrahedron Lett.* **1984**, *25*, 4337. (b) Seebach, D.; Fadel, A. *Helv. Chim. Acta* **1985**, *68*, 1243. (c) Seebach, D.; Aebi, J. D.; Gander-Coquoz, M.; Naef, R. *Helv. Chim. Acta* **1987**, *70*, 1194.

(20) (a) Beck, A. K.; Seebach, D. *Chimia* **1988**, *42*, 142. (b) Nebel, K.; Mutter, M. *Tetrahedron* **1988**, *44*, 4793.

(21) The alkylation of an imidazolidinone enolate with ethylene oxide in the presence of BF₃·OEt₂ (56% yield) has been reported: Fitzi, R.; Seebach, D. *Tetrahedron* **1988**, *44*, 5277.

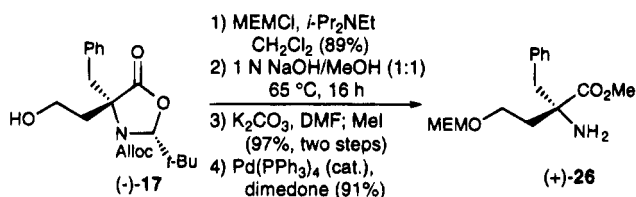


(22) Smith, A. B., III; Pasternak, A.; Yokoyama, A.; Hirschmann, R. *Tetrahedron Lett.* **1994**, *35*, 8977.

Table 1. Variation of Oxazolidinone and Epoxide Coupling Partners

Entry	Oxazolidinone	Epoxide	Product	Yield (%)	Selectivity (de)
1				69	≥95
2	(-)-9		(+)-17 $[\alpha]_D^{25} +42^\circ$	68	≥95
3				47	≥95
4				54	89
5				64	≥95
6	(-)-9			40	≥95
7 ²³	(-)-9			48	≥95 (each isomer)
8	(-)-9		—	NR	—

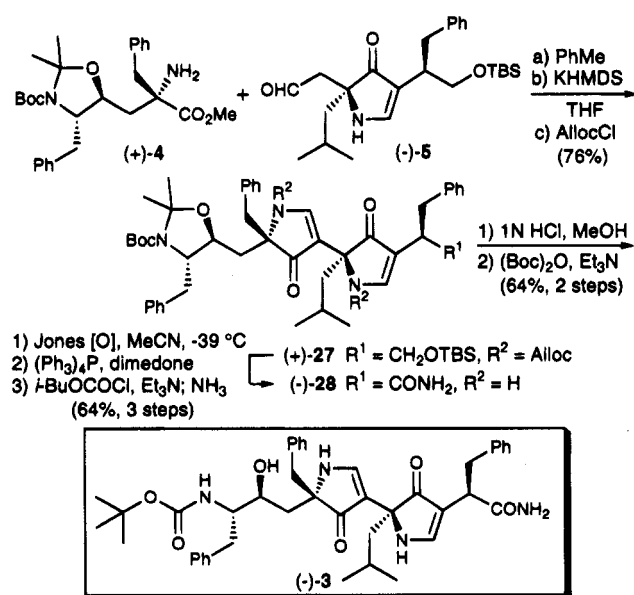
Scheme 4



acetone in **28** could be effected in the presence of the Boc group with CSA and ethylene glycol in methanol, but this alternative proved less efficient (39% yield).

Bioassay of 3: HIV-1 Protease Inhibition and Cellular Antiviral Activity. The enzyme inhibitory (IC_{50}) and cellular activated (CIC_{50}) assays were carried out via published procedures.²⁴ In enzyme inhibition the IC_{50} of **3** proved to be 10 nM, compared with 0.6 nM for the related peptidomimetic L-682,679; the results indicate that the bis(pyrrolinone) is recognized and bound by HIV-1 protease, but not as effectively as the peptide-based analog. Because one would expect the preorganization built into **3** to result in tighter binding to the enzyme, the explanation for the higher IC_{50} value actually observed has not yet been established but may reflect lower complementarity (i.e., displacement of the NHs or unfavorable steric interactions) with the active site for **3** relative to L-682,679. We anticipate that X-ray analysis now underway will clarify this point. Importantly, however, the relative potencies

Scheme 5



were reversed in the cellular antiviral assay (CIC_{95} values of 1.5 and 6.0 μ M, respectively), suggesting that bis(pyrrolinone) **3** is more readily transported into the cell than its peptidic counterpart. This conclusion emerges most clearly from the

ratios of CIC_{95} to IC_{50} (C/I). These values serve as an index of cell penetration, as antiviral activity requires transport of the inhibitor into the HIV-infected lymphocytes;^{24b} lower C/I ratios thus signify better cellular transport properties. The C/I ratios for **3** and L-682,679 were 150 and 10 000, respectively, the largest difference we have observed for a pyrrolinone-based/amide-based inhibitor pair.

We have proposed an explanation for the improved transport of our pyrrolinones vis-à-vis the corresponding peptide-based species^{1m,p} based upon the observation by Stein that cellular transport correlates inversely with the ability to H-bond intermolecularly with water.²⁵ He proposed that solvation is an impediment to transport because extraction of a molecule into a lipid bilayer from an aqueous phase requires desolvation, an endothermic process. In addition, Diamond and Wright presented evidence that an *intramolecular* hydrogen bond (as found in **3**) can lead to better transport by reducing the number of waters of solvation by two.²⁶ It is noteworthy that these concepts also serve to explain, at least in part, the unexpectedly favorable oral bioavailability of cyclosporin A. Seven of its amide bonds are methylated, and in hydrophobic solvents, the remaining four secondary amides participate in intramolecular H-bonding (three transannular H-bonds and one solvent exposed).²⁷ The latter conformation presumably is also adopted when cyclosporin passes through cell membranes, with the intramolecular hydrogen bonds reducing the required desolvation energy.²⁸

Analogs of Bis(pyrrolinone) 3: Synthesis and Biological Activity. To refine our understanding of the binding interactions in the HIV-1 protease active site and further improve the inhibitor transport properties, we next prepared a number of analogs of **3** (i.e., **33**, **35**, **36**, **39**, and **40**). Ghosh and co-workers³¹ replaced the Boc group on the P_1 amino functionality of inhibitor L-685,434 (**29**) with a carbamate derived from (*S*)-3-hydroxytetrahydrofuran, resulting in reductions of the IC_{50} and CIC_{95} values by 1 and 2 orders of magnitude, respectively (Figure 6). The analogous carbamate congener of **3** was prepared by treatment of (–)-**31**, the immediate synthetic precursor of (–)-**3** (Scheme 5, structure not shown), with the readily available 3-tetrahydrofuranyl succinimidyl carbonate (**32**) (Scheme 6).³² The resultant bis(pyrrolinone) (–)-**33** gave IC_{50} and CIC_{95} values of 1.3 and 800 nM. The order-of-magnitude improvement in IC_{50} , compared with **3**, mirrors the findings of Ghosh and confirms that the two classes of inhibitors have similar binding modes. This result was expected on the basis of our design strategy and molecular modeling, as well as the

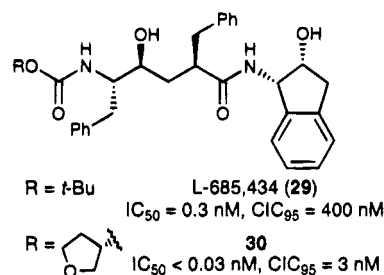
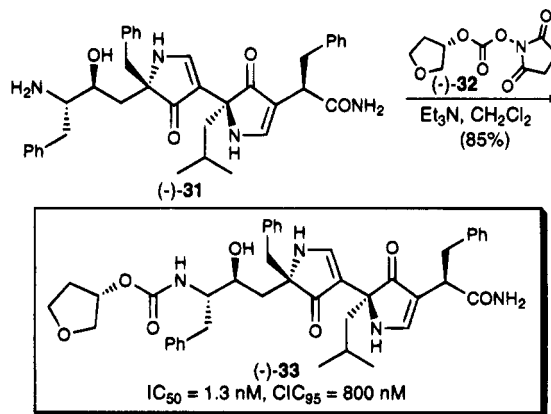


Figure 6. Enhanced activity attributable to the THF-derived N-terminal carbamate in a peptide-based inhibitor.

reported bound X-ray structure of an enzyme-bound inhibitor closely related to L-685,434.³³ In contrast, the CIC_{95} value for **33** did not show the same degree of improvement observed by Ghosh. The reasons for this discrepancy are not clear. The greater conformational flexibility of **29** might facilitate hydrophobic collapse³⁴ in an aqueous environment, shielding the tetrahydrofuranyl carbamate oxygens from solvation; reduced solvation might in turn lead to improved transport and better CIC_{95} values.

Scheme 6



Evaluation in two dogs revealed that **33** was not orally bioavailable in dogs. Its absence from the plasma could reflect nonabsorption from the gastrointestinal tract, first-pass metabolism in the liver, or excretion into the bile. Given the high molecular weight (735), lack of oral bioavailability was not unexpected. Consistent with this interpretation, we have recently synthesized a pyrrolinone-based HIV-1 protease inhibitor with a lower molecular weight (<600); this compound has proven to be orally bioavailable in dogs in preliminary experiments³⁵ and will be described in due course.

The improved in vitro potency of **33** encouraged us to explore other modifications based upon peptide SAR's, with particular emphasis on optimizing the C-terminus. The potency of HIV-1 protease inhibitors containing P_3' methyl ester³⁶ and *tert*-butyl amide³⁷ endcaps suggested the synthesis of **35** and **39**. Importantly, we anticipated that either of the latter endcaps would result in reduced solvation with water. We also sought to prepare the N-terminal (*S*)-3-hydroxytetrahydrofuranyl carbam-

(25) Stein, W. D. In *The Movement of Molecules Across Cell Membranes*; Academic: New York, 1967; pp 65–125.

(26) Diamond, J. M.; Wright, E. M. *Proc. R. Soc. B* **1969**, *172*, 273.

(27) (a) Kessler, H.; Loosli, H.-R.; Oschkinat, H. *Helv. Chim. Acta* **1985**, *68*, 661. (b) Kessler, H.; Gehrke, M.; Lautz, J.; Köck, M.; Seebach, D.; Thaler, A. *Biochem. Pharmacol.* **1990**, *40*, 169; erratum 2185.

(28) In contrast, a number of equilibrating conformations appear to be present in polar solvents such as DMSO-*d*₆²⁹ and in protic media.³⁰ It has been shown that binding to cyclophilin induces a conformational change in cyclosporin A: all of the intramolecular H-bonds are broken, and these functionalities become available for intermolecular interactions.²⁹

(29) (a) Fesik, S. W.; Gampe, R. T.; Holzman, T. F.; Egan, D. A.; Edalji, R.; Luly, J. R.; Simmer, R.; Helfrich, R.; Kishore, V.; Rich, D. H. *Science* **1990**, *250*, 1406. (b) Fesik, S. W.; Weber, C.; Wiber, B.; von Freyberg, B.; Traber, R.; Braun, W.; Widmer, H.; Wüthrich, K. *Biochemistry* **1991**, *30*, 6563. (c) Fesik, S. W.; Gampe, R. T., Jr.; Eaton, H. L.; Gemmecker, G.; Olejniczak, E. T.; Neri, P.; Holzman, T. F.; Egan, D. A.; Edalji, R.; Simmer, R.; Helfrich, R.; Hochlowski, J.; Jackson, M. *Biochemistry* **1991**, *30*, 6574.

(30) Kofron, J. L.; Kuzmic, P.; Kishore, V.; Gemmecker, G.; Fesik, S. W.; Rich, D. H. *J. Am. Chem. Soc.* **1992**, *114*, 2670.

(31) Ghosh, A. K.; Thompson, W. J.; McKee, S. P.; Duong, T. T.; Lyle, T. A.; Chen, J. C.; Darke, P. L.; Zugay, J. A.; Emini, E. A.; Schleif, W. A.; Huff, J. R.; Anderson, P. S. *J. Med. Chem.* **1993**, *36*, 292.

(32) Ghosh, A. K.; Duong, T. T.; McKee, S. P.; Thompson, W. J. *Tetrahedron Lett.* **1992**, *33*, 2781.

(33) Thompson, W. J.; Fitzgerald, P. M. D.; Holloway, M. K.; Emini, E. A.; Darke, P. L.; McKee, B. M.; Schleif, W. A.; Quintero, J. C.; Zugay, J. A.; Tucker, T. J.; Schwering, J. E.; Homnick, C. F.; Nunberg, J.; Springer, J. P.; Huff, J. R. *J. Med. Chem.* **1992**, *35*, 1685.

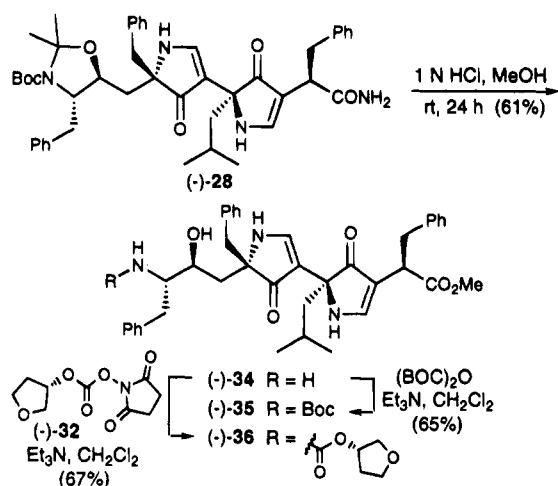
(34) (a) Wiley, R. A.; Rich, D. H. *Med. Res. Rev.* **1993**, *3*, 327. (b) Rich, D. H. In *Perspectives in Medicinal Chemistry*; Testa, B.; Kyburz, E.; Fuhrer, W., Giger, W., Eds.; VCH: New York, 1993.

(35) Pasternak, A. University of Pennsylvania. Unpublished results.

(36) Sigal, I. S.; et al. European Patent Application 0337714, 1988.

(37) Huff, J. R. Merck Research Laboratories, private communication.

Scheme 7

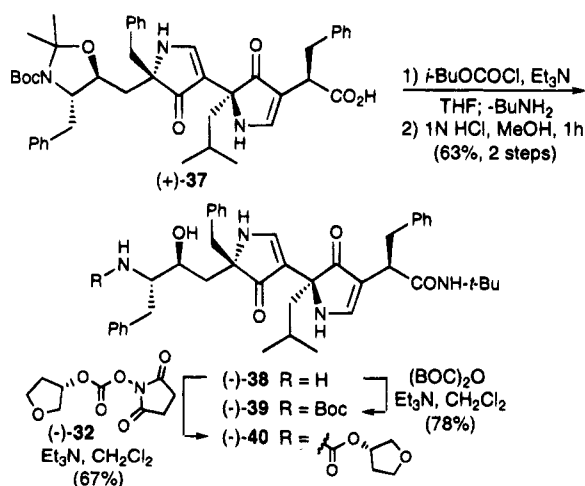


ate analogs embodying both the P_{3'} methyl ester and *tert*-butyl amide moieties (36 and 40, respectively).

Methyl esters 35 and 36 were elaborated from (-)-28 (Scheme 7). Exposure to acidic methanol at room temperature for 24 h resulted in removal of the Boc and acetonide groups as well as methanolysis of the C-terminal primary amide, furnishing amino ester (-)-34 in 61% yield. The latter unforeseen methanolysis reaction was relatively slow; after 1 h the fully deprotected primary amide could be isolated as the major product (Scheme 5). Amine 34 then furnished the Boc and 3-hydroxytetrahydrofuran carbamate analogs (-)-35 and (-)-36 by treatment with (Boc)₂O (65% yield) and (-)-3-tetrahydrofuran succinimidyl carbonate (32) (67%).

For the synthesis of *tert*-butyl amides 39 and 40, we turned to carboxylic acid (+)-37, also an intermediate in the synthesis of 3 (Scheme 5, structure not shown). Amide formation via a mixed anhydride (81% yield), followed by simultaneous Boc and acetonide removal (78%) provided primary amine (-)-38 (Scheme 8), which was converted to the Boc and 3-(*S*)-hydroxytetrahydrofuran carbamates (-)-39 (78% yield) and (-)-40 (67%) as described for 35 and 36.

Scheme 8



HIV-1 Protease Inhibition and Antiviral Activity of 35, 36, 39, and 40. Bioassay results for all of the bis(pyrrolinones) are compared with the data for peptidal inhibitor L-682,679 in Table 2. The P_{3'} *tert*-butyl amide and methyl ester endcaps led to somewhat diminished potency in enzyme inhibition (IC₅₀) compared with the original primary amides. In both the Boc and 3-hydroxy THF series, the methyl ester analogs were slightly

Table 2. Bioassay Data: Inhibition of HIV-1 Protease (IC₅₀), Cellular Antiviral Activity (CIC₉₅), and C/I Ratios

inhibitor	N-terminus	C-terminus	IC ₅₀ (nM)	CIC ₉₅ (nM)	C/I
L-682,679	Boc	NH ₂	0.6	6000	10000
3	Boc	NH ₂	10	1500	150
35	Boc	OMe	37		
39	Boc	NH- <i>t</i> -Bu	48		
33	furanyl carbamate	NH ₂	1.3	800	615
36	furanyl carbamate	OMe	2.0	400	200
40	furanyl carbamate	NH- <i>t</i> -Bu	3.3	800	242

more active than the *tert*-butyl amides. No analogous SAR's are available for the peptidal inhibitor L-682,679, precluding a direct SAR correlation with the pyrrolinone-based structures. We note, however, that in all cases replacement of the N-terminal Boc group with an (*S*)-3-hydroxytetrahydrofuran urethane resulted in an order-of-magnitude decrease in the IC₅₀ value.

Importantly, in the furanyl carbamate series the C-terminal *tert*-butyl amide 40 proved to be as active as the corresponding primary amide 33 in the cellular assay (CIC₉₅); moreover, methyl ester 36 gave the lowest value we have observed to date. The superior (i.e., lower) C/I ratios for these two compounds compared with primary amide 33, indicate that the two new C-terminal endcaps result in improved transport properties.

Summary and Conclusions. Inhibitors incorporating our pyrrolinone-based, non-peptidal β -strand motif inhibit the HIV-1 protease. The bis(pyrrolinones) described herein are more active than a related peptidal structure in cellular antiviral assays despite displaying lower potency in enzyme inhibition; the lower CIC₉₅/IC₅₀ ratios are attributed to decreased solvation of the pyrrolinones compared with the corresponding peptides. We are currently evaluating the pharmacokinetic properties of pyrrolinone-based inhibitors with lower molecular weights.

Replacement of the N-terminal Boc group with a carbamate derived from (*S*)-3-hydroxytetrahydrofuran improved enzyme inhibition and antiviral activity in all cases. This observation is in accord with published SAR studies for peptide-derived inhibitors and thus may provide additional evidence for analogous modes of enzyme-inhibitor binding. To buttress this important inference we are attempting to determine the X-ray crystal structure of HIV-1 protease cocrystallized with inhibitor 33. Incorporation of a methyl ester or *tert*-butyl amide in place of the C-terminal primary amide generated pyrrolinone inhibitors with identical or improved antiviral activities (CIC₉₅) and enhanced transport properties, the latter revealed by the C/I ratios.

Finally, our success in employing pyrrolinone-based, non-peptide peptidomimetics to inhibit both HIV-1 protease and renin suggests that the pyrrolinones will prove to be broadly useful as mimics of peptidal β -strands.

Experimental Section³⁸

Oxazolidinone (+)-11. A solution of (*S*)-(-)-4-benzyl-2,5-oxazolidinone (10)¹⁶ (25.00 g, 141.1 mmol) in THF (500 mL) was cooled to -78 °C and treated dropwise over ca. 45 min with *n*-BuLi (2.5 M in hexane, 56.4 mL, 141 mmol). The resultant yellow solution was stirred for an additional 10 min and neat hydrocinnamoyl chloride (23.8 g, 21.0 mL, 141 mmol) was added dropwise over ca. 15 min. The reaction mixture was stirred 15 min further at -78 °C and then warmed to room temperature. After 1 h the mixture was diluted with Et₂O (600 mL) and washed with saturated aqueous NaHCO₃ (3 × 200 mL) and brine (200 mL). The organic phase was dried over MgSO₄, filtered, and

concentrated. Flash chromatography (gradient elution, 5–20% EtOAc/hexanes) furnished the hydrocinnamoyl oxazolidinone (33.72 g, 77% yield) as white needles. Crystallization of an analytical sample from hot EtOAc/hexanes gave a white solid: mp 106.5–107.5 °C.

At –78 °C a solution of the hydrocinnamoyl oxazolidinone (33.7 g, 109 mmol) in THF (500 mL) was treated over ca. 1 h with NaHMDS (1.0 M in THF, 131 mL, 131 mmol). The mixture was stirred 15 min further, and freshly distilled prenyl bromide (48.7 g, 37.7 mL, 0.327 mol) was added dropwise over ca. 30 min. After an additional 15 min at –78 °C, the reaction was warmed to 0 °C, stirred for 45 min, and poured into 10% aqueous NaHSO₄ (300 mL). After separation of the layers, the aqueous phase was extracted with EtOAc (2 × 250 mL) and the combined organic layers were washed with 10% aqueous NaHSO₄, saturated aqueous NaHCO₃, and brine (200 mL each), dried over MgSO₄, filtered, and concentrated. Flash chromatography (10% EtOAc/hexanes) afforded **11** (32.8 g, 80% yield) as a white solid, an analytical sample of which could be crystallized from hot EtOAc/hexanes to give white needles: mp 78.5–80 °C; $[\alpha]_D^{25} +120^\circ$ (c 1.03, CHCl₃); ¹³C NMR (62.5 MHz, CDCl₃) δ 175.7, 152.9, 139.2, 135.2, 134.1, 129.3, 129.0, 128.0, 128.2, 127.2, 126.2, 120.7, 65.6, 55.2, 44.6, 38.1, 37.7, 30.8, 25.8, 17.8; HRMS (FAB, NBA) m/z 378.2057 [(M + H)⁺; calcd for C₂₄H₂₈NO₃ 378.2069]. Anal. Calcd for C₂₄H₂₇NO₃: C, 76.36; H, 7.22; N, 3.71. Found: C, 76.45; H, 7.62; N, 4.00.

Alcohol (+)-12. *n*-BuLi (2.5 M in hexane, 9.5 mL, 23.8 mmol) was slowly added to a solution of BnSH (3.92 g, 3.7 mL, 31.8 mmol) in THF (120 mL) at 0 °C. The resultant mixture was transferred dropwise via a cannula to a solution of oxazolidinone (+)-**11** (6.00 g, 15.9 mmol) in THF (240 mL) cooled to 0 °C. After an additional 15 min LAH (1.0 M in THF, 23.8 mL, 23.8 mmol) was added dropwise. The reaction mixture was stirred 0.5 h further at 0 °C, quenched by sequential addition of H₂O (1 mL), 10% aqueous NaOH (2 mL), and H₂O (2 mL), stirred for 0.5 h at room temperature, filtered, and concentrated. Flash chromatography (10% EtOAc/hexanes) afforded **12** (3.24 g, 100% yield) as a colorless liquid. The oxazolidinone auxiliary was also recovered (2.33 g, 83%).

12: $[\alpha]_D^{24} +27^\circ$ (c 1.0, CHCl₃); ¹³C NMR (62.5 MHz, CDCl₃) δ 140.7, 133.2, 129.1, 128.2, 125.8, 122.3, 65.1, 43.3, 37.5, 29.5, 25.8, 17.8; HRMS (CI, NH₃) m/z 204.1495 [M⁺; calcd for C₁₄H₂₀O 204.1514].

Silyloxy Aldehyde (–)-7. A solution of alcohol (+)-**12** (3.59 g, 17.6 mmol) in DMF (30 mL) was treated with imidazole (2.99 g, 43.9 mmol) and TBSCl (3.18 g, 21.1 mmol) and stirred overnight at ambient temperature. The reaction mixture was then partitioned between Et₂O (200 mL) and H₂O (500 mL) and the aqueous phase extracted with Et₂O (100 mL). The combined organic solutions were dried over MgSO₄, filtered, and concentrated. Flash chromatography (2% Et₂O/

hexanes) furnished the silyl ether (5.45 g, 97% yield) as a colorless liquid.

Ozone was bubbled through a solution of the silyl ether (4.85 g, 15.2 mmol) in CH₂Cl₂ (100 mL) at –78 °C until a pale blue color persisted. Argon was then passed through the solution until the blue color disappeared. Ph₃P (4.00 g, 15.2 mmol) was added and the reaction mixture allowed to warm to room temperature, stirred overnight, and concentrated. Flash chromatography (5% Et₂O/petroleum ether) afforded **7** (4.06 g, 91% yield) as a colorless oil: $[\alpha]_D^{25} +10^\circ$ (c 1.0, CHCl₃); ¹³C NMR (62.5 MHz, CDCl₃) δ 202.3, 139.6, 129.2, 128.4, 126.2, 65.0, 45.8, 38.3, 37.3, 25.7, 18.2, –5.5; HRMS (FAB, NBA) m/z 293.1942 [(M + H)⁺; calcd for C₁₇H₂₈O₂Si 293.1937]. Anal. Calcd for C₁₇H₂₈O₂Si: C, 69.79; H, 9.67. Found: C, 69.39; H, 9.93.

Mono(pyrrolinone) (–)-7. Amino ester (+)-**6** (15.2 g, 71.2 mmol) and aldehyde (–)-**7** (20.5 g, 70.0 mmol) were dissolved in CHCl₃ (100 mL) and toluene (200 mL) at ambient temperature. The resultant solution was allowed to stand for 15 min and then concentrated in vacuo. The residue was then redissolved in toluene (200 mL) and the solution concentrated; this cycle was repeated four times. Following final concentration under high vacuum for 0.5 h, the crude imine was dissolved in THF (550 mL) and KHMDS (0.5 M in toluene, 574 mL, 287 mmol) was slowly added (20 min). During the addition the color of the reaction mixture changed from pale yellow to orange. The mixture was stirred 20 min further, cooled to 0 °C, and treated with neat AllocCl (45.3 mL, 51.5 g, 427 mmol) over 10 min. After an additional 25 min, the mixture was poured into 10% aqueous NaHSO₄ (500 mL), the phases were separated, and the aqueous layer was washed with Et₂O (2 × 400 mL). The combined organic solutions were washed with brine (400 mL), dried over MgSO₄, filtered, and concentrated. Flash chromatography (5% EtOAc/hexanes) gave **13** (27.9 g, 74% yield) as a pale yellow oil. NMR data were acquired at 350 K to achieve coalescence of the resonances for two rotamers observable at ambient temperature: $[\alpha]_D^{26} -44^\circ$ (c 1.0, CHCl₃); ¹³C NMR (125 MHz, DMSO-*d*₆, 350 K) δ 202.5, 156.2, 152.7, 139.3, 134.3, 131.8, 128.2, 127.6, 125.4, 122.0, 118 (br), 115.8, 71.5, 65.8, 63.2, 43.7 (br), 36.8, 35.2, 25.3, 24.9, 23.5, 23.2, 22.8, 17.4, 17.1, –6.0; HRMS (FAB, NBA) m/z 540.3483 [(M + H)⁺; calcd for C₃₂H₅₀NO₄Si 540.3509]. Anal. Calcd for C₃₂H₄₉NO₄Si: C, 71.18; H, 9.17; N, 2.60. Found: C, 70.98; H, 9.39; N, 2.39.

Aldehyde (–)-5. A solution of Alloc-protected prenyl oxazolidinone (–)-**13** (1.31 g, 2.43 mmol) in acetone and H₂O (4:1, 75 mL) was treated with NMO (1.14 g, 9.72 mmol) and a few crystals of OsO₄. The reaction mixture was stirred at room temperature for 48 h, quenched with 10% aqueous NaHSO₃ (10 mL), and stirred 15 min further. Most of the acetone was then removed under reduced pressure and the resultant aqueous solution extracted with EtOAc (3 × 75 mL). The combined organic layers were washed with 10% aqueous NaHSO₃ and brine (75 mL each), dried over MgSO₄, filtered, and concentrated. The crude tetraols were dissolved in *p*-dioxane and 2% aqueous NaOH (1:1 135 mL) precooled to 0 °C. The reaction mixture was stirred at 0 °C for 1 h, and the pH was then adjusted to <7 by slow addition of 10% aqueous NaHSO₄. Following extraction with Et₂O (3 × 75 mL), the combined organic phases were washed with brine (75 mL), dried over MgSO₄, filtered, and concentrated. Flash chromatography (50% EtOAc/hexanes) gave a mixture (ca. 1:1) of diastereomeric diols (1.01 g, 85% yield) as an oil. This material was then dissolved in CH₂Cl₂ (15 mL) and treated at 0 °C with anhydrous K₂CO₃ (0.761 g, 5.51 mmol) and Pb(OAc)₄ (1.13 g, 2.55 mmol). After 20 min, the reaction mixture was partitioned between H₂O (75 mL) and EtOAc (100 mL) and the aqueous phase was extracted with EtOAc (100 mL). The combined organic solutions were washed with saturated aqueous NaHCO₃ (2 × 75 mL), dried over MgSO₄, filtered, and concentrated. Flash chromatography (40% EtOAc/hexanes) furnished **5** (664.1 mg, 76% yield, 65% for the three steps) as a pale yellow oil which darkened upon storage: $[\alpha]_D^{25} -57^\circ$ (c 2.6, CHCl₃); ¹³C NMR (62.5 MHz, CDCl₃) δ 202.3, 200.4, 161.7, 140.4, 129.2, 128.1, 125.8, 113.3, 67.3, 64.1, 50.3, 44.3, 37.2, 36.7, 26.0, 24.4, 24.2, 24.0, 18.2, –5.4, –5.5; HRMS (FAB, NBA) m/z 430.2754 [(M + H)⁺; calcd for C₂₅H₄₀NO₃Si 430.2777].

β -Hydroxy Oxazolidinone (–)-16. A solution of oxazolidinone (+)-**9** (3.60 g, 11.3 mmol) in THF (55 mL) was cooled to –78 °C, and KHMDS (0.5 M toluene, 49.9 mL, 25.0 mmol) was carefully added dropwise such that the internal reaction temperature did not exceed

(38) **Materials and Methods.** All reactions were carried out under argon with dry, freshly distilled solvents, in vacuum-flamed glassware with magnetic stirring, except as otherwise indicated. Diethyl ether (Et₂O) and tetrahydrofuran (THF), benzene and toluene, and dichloromethane (CH₂Cl₂) were distilled from sodium/benzophenone, sodium, and calcium hydride, respectively. Triethylamine, diisopropylethylamine, and pyridine were distilled from calcium hydride and stored over KOH. *n*-Butyllithium was standardized by titration with diphenylacetic acid.

All reactions were monitored by thin layer chromatography (TLC) with 0.25-mm E. Merck precoated silica gel plates. Flash chromatography was performed with the indicated solvents and E. Merck silica gel 60 (particle size 0.040–0.063 mm). Yields refer to chromatographically and spectroscopically pure compounds, unless otherwise indicated.

All melting points were determined with a Thomas-Hoover apparatus and are corrected. Infrared spectra were recorded on a Perkin-Elmer Model 283B spectrophotometer. Proton and carbon-13 NMR spectra were recorded on a Bruker AM-500 spectrometer and a Bruker WH-250 or WH-500 instrument, respectively. Chemical shifts are reported in δ values relative to tetramethylsilane. Optical rotations were measured with a Perkin-Elmer Model 241 polarimeter. High-resolution mass spectra were obtained at the University of Pennsylvania Mass Spectrometry Center with either a VG Micromass 70/70H or VG ZAB-E spectrometer. High-performance liquid chromatography was performed with a Rainin system equipped with a Dynamax Method Manager, Rabbit MPX solvent delivery system, Rheodyne injector, and Gilson Model 131 refractive index detector or Gilson Model 115 variable-wavelength UV detector. Normal-phase columns, 4.0, 10.0, or 25.0 mm × 25 cm with 8- μ m (60 Å) packing, were purchased from Dynamax.

Microanalyses were performed by Robertson Labs, Madison, NJ.

−74 °C. After an additional 10 min, a solution of epoxide (+)-**14**¹⁸ (3.43 g, 13.0 mmol) in THF (5 mL) was added in the same fashion. The reaction was stirred 15 min further, Et₂AlCl (1.0 M in heptane, 79.4 mL, 79.4 mmol) was added dropwise, and after another 10 min, the mixture was poured into a mixture of ice and 1 N HCl (1:1, 100 mL). Following extraction with EtOAc (3 × 75 mL), the combined organic layers were washed with 1 N HCl and brine (75 mL each), dried over MgSO₄, filtered, and concentrated. Flash chromatography (gradient elution, 10–25% EtOAc/hexanes) afforded **16** (4.07 g, 62% yield) as a white powder. NMR analysis at 330 K coalesced the rotameric signals observed at ambient temperature: mp 60–62 °C; [α]_D²⁵ −51.1° (c 1.93, CDCl₃); ¹³C NMR (125 MHz, CDCl₃, 330 K) δ 173.8, 156.4, 155.2, 138.0, 135.6, 132.2, 131.2, 129.2, 128.6, 128.3, 127.2, 126.5, 119.1, 95.6, 79.8, 69.8, 67.6, 66.5, 58.0, 43.4, 39.9, 37.8 (br), 37.6, 28.3, 25.3; HRMS (FAB, NBA) *m/z* 581.3224 [(M + H)⁺; calcd for C₃₃H₄₅N₂O₇ 581.3226]. Anal. Calcd for C₃₃H₄₅N₂O₇: C, 68.24; H, 7.65; N, 4.82. Found: C, 67.89; H, 7.40; N, 4.70.

Acetonide α-Amino Ester (+)-4. β-Hydroxy oxazolidinone (−)-**16** (12.8 g, 22.0 mmol) was dissolved in acetone and Me₂C(OMe)₂ (1:1, 400 mL). *p*-TsOH·H₂O (100 mg, 0.53 mmol) was added, the mixture was stirred at room temperature for 3 days, and the solution was then concentrated under reduced pressure without heating. Flash chromatography (gradient elution, 10–20% EtOAc/hexanes) gave the intermediate acetonide (12.4 g, 91% yield) as a white foam consisting of two rotameric isomers.

A solution of the oxazolidinone acetonide (0.860 g, 1.39 mmol) in MeOH (15 mL) was treated with 1 N methanolic NaOH (15 mL) and heated at reflux for 3 days. Most of the MeOH was evaporated, and the resultant aqueous mixture was acidified to pH 3 with 10% aqueous NaHSO₄ and then extracted with EtOAc (3 × 60 mL). The combined organic layers were washed with brine (60 mL), dried over MgSO₄, filtered, and concentrated. The crude acid was dissolved in DMF (20 mL), and anhydrous K₂CO₃ (0.574 g, 4.16 mmol) was added. The suspension was cooled to 0 °C and treated with MeI (393 mg, 0.172 mmol, 2.77 mmol). The reaction mixture was stirred for an additional 20 min at 0 °C and 1 h at room temperature and then was partitioned between Et₂O (100 mL) and H₂O (50 mL). The aqueous phase was extracted with Et₂O (100 mL), and the combined ethereal solutions were washed with H₂O (3 × 75 mL), saturated aqueous NaHCO₃, and brine (75 mL each), dried over MgSO₄, filtered, and concentrated. Flash chromatography (20% EtOAc/hexanes) furnished the intermediate methyl ester (699 mg, 89% yield) as a colorless glass.

A mixture of the Alloc-protected amino ester (8.50 g, 15.0 mmol), dimedone (10.5 g, 75.0 mmol), Pd(PPh₃)₄ (175 mg, 0.151 mmol), and THF (100 mL) was stirred at room temperature overnight and then partitioned between 10% aqueous NaOH and Et₂O (100 mL each). The aqueous phase was extracted with Et₂O (2 × 100 mL), and the combined organic solutions were washed with 10% aqueous NaOH (2 × 100 mL), H₂O, and brine (100 mL each), dried over MgSO₄, filtered, and concentrated. Flash chromatography (30% EtOAc/hexanes) afforded **4** (6.98 g, 96% yield) as a pale yellow viscous oil. NMR analysis at 320 K coalesced most of the rotameric signals observed at ambient temperature: [α]_D²⁵ +17° (c 1.0, CHCl₃); ¹³C NMR (125 MHz, CDCl₃, 320 K) δ 176.6, 152.0 (br), 137.4, 136.5, 129.9, 128.3, 128.2, 126.8, 126.5, 94.5 (br), 80.0, 75.9 (br), 64.0, 62.2, 51.7, 47.0, 43.8 (br), 39 (br), 36.4 (br), 28.5, 26.4; HRMS (FAB, NBA) *m/z* 483.2874 [(M + H)⁺; calcd for C₂₈H₃₉N₂O₅ 483.2859]. Anal. Calcd for C₂₈H₃₉N₂O₅: C, 69.67; H, 7.95; N, 5.81. Found: C, 69.50; H, 8.06; N, 5.60.

General Procedure for Alkylation of Oxazolidinones with Epoxides Mediated by Lewis Acids (Table 1). **Alcohol (−)-17.** In a representative experiment, a solution of oxazolidinone (+)-**9** (162.7 mg, 0.513 mmol) in dry toluene (5 mL, ca. 0.1 M) was cooled to −78 °C and treated with KHMDS (0.5 N in toluene, 1.15 mL, 0.575 mmol). The reaction mixture was stirred for 20 min, Et₂AlCl (1.0 M in heptane, 1.10 mL, 1.10 mmol) was added dropwise, and the solution was stirred 15 min further. Excess ethylene oxide was then introduced via a balloon and the reaction stirred for an additional 1.5 h. Solid Na₂SO₄·10H₂O (ca. 5 g), NaHCO₃ (ca. 100 mg), and Et₂O (20 mL) were added at 78 °C, and the resultant suspension was stirred for 1 h at ambient temperature, filtered, and concentrated. Flash chromatography (1:6 EtOAc/hexanes to elute unreacted **9**, then 1:2 EtOAc/hexanes) afforded **17** (127.8 mg, 69% yield) as a colorless oil: [α]_D²⁵ −38° (c 1.1,

CHCl₃); ¹³C NMR (125 MHz, CDCl₃) δ 174.1; 155.2 (br), 135.5, 131.7, 131.1, 128.2, 127.2, 119.6, 95.3, 66.7, 66.4, 58.3, 43.1, 38.4 (br), 37.6, 25.3; HRMS (CI, NH₃) *m/z* 362.1973 [(M + H)⁺; calcd for C₂₀H₂₈NO₅ 362.1967].

The same reaction carried out with 1.1 and 3.1 equiv of Et₂AlCl gave (−)-**17** in 36% and 69% yields, respectively. With THF as the reaction solvent and 2.1 equiv of Et₂AlCl, (−)-**17** was formed in 32% yield.

Alcohol (+)-17: [α]_D²⁵ +42.0° (c 1.07, CHCl₃); ¹³C NMR (125 MHz, CDCl₃) δ 174.1, 155.0 (br), 135.4, 131.6, 131.0, 128.2, 127.2, 119.5, 95.3, 66.6, 66.4, 58.1, 43.1, 38.8 (br), 37.6, 25.2; HRMS (CI, NH₃) *m/z* 362.1958 [(M + H)⁺; calcd for C₂₀H₂₈NO₅ 362.1967]. Anal. Calcd for C₂₀H₂₇NO₅: C, 66.46; H, 7.53; N, 3.81. Found: C, 66.07; H, 7.81; N, 3.81.

Alcohol (+)-19: [α]_D²⁵ +15.7° (c 1.07, CHCl₃); ¹³C NMR (125 MHz, CDCl₃) δ 174.8, 155.1, 131.7, 119.4, 94.9, 67.0, 66.6, 58.6, 37.6, 36.1, 32.1, 26.0, 18.7, 18.1; HRMS (CI, NH₃) *m/z* 314.1965 [(M + H)⁺; calcd for C₁₆H₂₈NO₅ 314.1967]. Anal. Calcd for C₁₆H₂₇NO₅: C, 61.32; H, 8.68; N, 4.47. Found: C, 61.20; H, 9.03; N, 4.37.

Alcohol (+)-21: [α]_D²⁵ +5.4° (c 1.05, CHCl₃); ¹³C NMR (125 MHz, CDCl₃) δ 175.1, 154.6 (br), 131.7, 119.3, 95.0, 66.5, 64.7, 58.3, 47.0, 37.8, 37.7 (br), 25.8, 24.9, 24.6, 23.5; HRMS (CI, NH₃) *m/z* 328.2141 [(M + H)⁺; calcd for C₁₇H₃₀NO₅ 328.2124].

Alcohol (+)-23: [α]_D²⁵ +18.8° (c 1.02, CHCl₃); ¹³C NMR (125 MHz, CDCl₃) δ 175.8, 155.0 (br), 131.7, 118.9, 94.9, 66.3, 61.4, 58.1 (br), 40.0 (br), 38.2 (br), 25.32, 25.30 (br); HRMS (CI, NH₃) *m/z* 286.1652 [(M + H)⁺; calcd for C₁₄H₂₄NO₅ 286.1654]. Anal. Calcd for C₁₄H₂₃NO₅: C, 58.93; H, 8.12; N, 4.91. Found: C, 58.76; H, 7.89; N, 4.65.

Alcohol (+)-24: [α]_D²⁵ +14.2° (c 1.32, CHCl₃); ¹³C NMR (125 MHz, CDCl₃) δ 174.2, 154.8 (br), 137.6, 135.4, 131.5, 131.1, 128.4, 128.2, 127.9, 127.7, 127.2, 119.8, 95.2, 73.7, 66.6 (2 C), 65.4, 43.7, 40.2 (br), 37.6, 25.5; HRMS (CI, NH₃) *m/z* 499.2808 [(M + NH₄)⁺; calcd for C₂₈H₃₉N₂O₆ 499.2808].

Alcohol 25b: [α]_D²⁵ +59° (c 0.94, CHCl₃); ¹³C NMR (125 MHz, CDCl₃) δ 173.8, 155.8 (br), 135.6, 132.1, 131.1, 128.2, 127.2, 119.0, 95.7, 67.9, 66.4, 64.7, 43.3 (br), 43.2, 37.6, 25.5, 25.2; HRMS (CI, NH₃) *m/z* 376.2126 [(M + H)⁺; calcd for C₂₁H₃₀NO₅ 376.2124].

Alcohol 25a: [α]_D²⁵ +20.6° (c 1.06, CHCl₃); ¹³C NMR (125 MHz, CDCl₃) δ 174.7, 155.0 (br), 135.4, 131.5, 131.1, 128.2, 127.1, 119.8, 95.2, 66.6, 65.7, 64.2, 46.0 (br), 43.6, 37.5, 25.5, 24.4; HRMS (CI, NH₃) *m/z* 393.2381 [(M + NH₄)⁺; calcd for C₂₁H₃₃N₂O₅ 393.2390]. Anal. Calcd for C₂₁H₂₉NO₅: C, 67.18; H, 7.78; N, 3.73. Found: C, 67.07; H, 7.95; N, 3.64.

MEM-Protected α-Amino Ester (+)-26. At room temperature *i*-Pr₃NEt (141.4 mg, 190 μL, 1.10 mmol) and (MEM)Cl (90.9 mg, 0.730 mmol) were added to a solution of alcohol (−)-**17** (131.8 mg, 0.365 mmol) in dry CH₂Cl₂ (5 mL). The mixture was stirred for 19 h and then poured into Et₂O (50 mL), washed with brine (2 × 20 mL), dried over MgSO₄, filtered, and concentrated. Flash chromatography (1:3 EtOAc/hexanes) gave the MEM ether (145.5 mg, 89% yield) as a colorless oil.

A solution of the MEM ether (143.5 mg, 0.319 mmol) in MeOH (3 mL) was treated with aqueous NaOH (1 N, 3 mL) and stirred at 60 °C for 20 h. The reaction mixture was acidified to pH 3 with 3 N HCl, and brine (50 mL) was added followed by extraction with EtOAc (3 × 15 mL); the combined organic solutions were washed with brine (20 mL), dried over MgSO₄, filtered, and concentrated. A solution of the crude residue in DMF (1 mL) was cooled to 0 °C, treated with K₂CO₃ (161 mg, 0.96 mmol) and MeI (91 mg, 0.64 mmol), and stirred for 30 min at 0 °C and 45 min at room temperature. Aqueous NH₄Cl (10%, 5 mL) was then added, the mixture was extracted with EtOAc (3 × 5 mL), and the combined organic solutions were washed with brine (20 mL), dried over MgSO₄, filtered, and concentrated. Flash chromatography (1:2 EtOAc/hexanes) gave the methyl ester (118.3 mg, 94% yield) as a colorless oil.

At room temperature, dimedone (186 mg, 1.33 mmol) and Pd(PPh₃)₄ (12.2 mg, 0.0110 mmol) were added to a solution of the Alloc-protected α-amino ester (79.5 mg, 0.202 mmol) in THF (5 mL) and the resultant mixture was stirred for 17 h. The mixture was then poured into 10% aqueous NaOH (10 mL) and extracted with Et₂O (3 × 10 mL), and the combined organic layers were washed with 10% aqueous NaOH

(2 × 10 mL), distilled H₂O, and brine (10 mL each), dried over MgSO₄, filtered, and concentrated. Flash chromatography (gradient elution, 0–5% MeOH/EtOAc) afforded **26** (56.9 mg, 91% yield) as a colorless oil: $[\alpha]_D^{25} +10.1^\circ$ (c 1.04, CHCl₃); ¹³C NMR (125 MHz, CDCl₃) δ 176.7 (s), 135.9 (s), 129.9 (d), 128.3 (d), 126.9 (d), 95.3 (t), 71.7 (t), 66.8 (t), 63.8 (t), 61.0 (s), 58.9 (q), 51.8 (q), 46.7 (t), 39.3 (t); HRMS (CI, NH₃) *m/z* 312.1802 [(M + H)⁺; calcd for C₁₆H₂₆NO₅ 312.1811].

Bis(pyrrolinone) (+)-27. At room temperature, α-amino ester (+)-**4** (630.0 mg, 1.305 mmol) and aldehyde (–)-**5** (609.2 mg, 1.418 mmol) were dissolved in CHCl₃ (50 mL), toluene (200 mL) was added, and the solution was allowed to stand for 15 min and then concentrated under reduced pressure. The residue was redissolved in toluene (200 mL) and the solution concentrated; this cycle was repeated four times. Following final concentration under high vacuum for 1 h, the resultant imine was dissolved in THF (35 mL) and treated at room temperature dropwise with KHMDs (0.5 M in toluene, 10.4 mL, 5.22 mmol). After 15 min, the temperature was lowered to 0 °C and AllocCl (1.10 g, 0.970 mL, 9.14 mmol) was added dropwise. The reaction mixture was stirred 15 min further, poured into 10% aqueous NaHSO₄ (100 mL), and extracted with EtOAc (3 × 75 mL). The combined organic layers were washed with brine (100 mL), dried over MgSO₄, filtered, and concentrated. Flash chromatography (25% EtOAc/hexanes) provided **27** (1.03 g, 76% yield) as a colorless oil which became a puffy solid upon storing under vacuum. NMR signals of rotameric isomers coalesced almost completely at 355 K: mp 59–61 °C; $[\alpha]_D^{26} +52.8^\circ$ (c 1.04, CHCl₃); ¹³C NMR (125 MHz, DMSO-*d*₆, 355 K) δ 198.2, 197.7, 156.5 (br), 153.6, 150.9, 148.1 (br), 139.3, 136.8, 135.9 (br), 133.3, 131.7, 131.6, 130.3, 128.9, 128.6, 128.4, 127.74, 127.66, 127.2, 126.1, 125.8, 125.4, 121.4, 118.0, 117.9, 93.1, 78.9, 75.0, 71.5, 68.0, 66.8, 66.1, 65.8, 63.4, 63.0, 62.4, 41.7, 41.5, 37.0, 35.3, 27.7, 26.9, 25.3, 23.6, 22.8, 22.2, 21.8, 21.7, 17.4, –6.0, –6.1; HRMS (FAB, NBA) *m/z* 1030.5663 [(M + H)⁺; calcd for C₆₀H₇₉N₃O₁₀Si 1030.5612]. Anal. Calcd for C₆₀H₇₉N₃O₁₀Si: C, 69.93; H, 7.74; N, 4.08. Found: C, 69.87; H, 7.85; N, 3.96.

Carboxylic Acid (+)-37. A solution of silyl ether (+)-**27** (2.88 g, 2.79 mmol) in MeCN (1 L) was cooled to –40 °C (dry ice/MeCN bath), and Jones reagent (8 N, 5.53 mL, 44.3 mmol) was added dropwise. The reaction mixture was stirred at –40 °C for 4 h, quenched with *i*-PrOH (5 mL), poured into brine (1 L), and extracted with EtOAc (3 × 750 mL). The combined organic phases were washed with 10% aqueous NaHSO₃ (2 × 500 mL) and brine (500 mL), dried over MgSO₄, filtered, and concentrated. Flash chromatography (gradient elution, 1–3% MeOH/CH₂Cl₂) provided bis(Alloc)-protected acid (1.85 g, 71% yield) as a pale yellow glass.

A solution of the bis(Alloc)-protected acid (77.1 mg, 0.0829 mmol), dimesone (116 mg, 0.829 mmol), and Pd(PPh₃)₄ (ca. 5–10 mg) in THF (2 mL) was stirred at room temperature for 24 h, diluted with Et₂O (30 mL), and filtered through a Celite plug. The filter cake was washed with Et₂O (30 mL). Concentration and flash chromatography (0.5% HOAc, 49.5% EtOAc/hexanes) afforded the deprotected acid **37** (53.5 mg, 85% yield) as a white solid. NMR analysis at 330 K coalesced the rotameric signals observed at ambient temperature: mp 93 °C (dec); $[\alpha]_D^{25} -114^\circ$ (c 1.01, CHCl₃); ¹³C NMR (125 MHz, CDCl₃, 330 K) δ 202.2, 201.8, 174.8, 163.2, 161.4, 152.0, 138.5, 137.1, 134.4, 130.0, 129.7, 129.0, 128.5, 128.4, 128.2, 127.6, 127.1, 126.7, 126.5, 125.3, 109.9, 107.2, 94.5, 80.2, 75.0, 70.6, 68.9, 64.0, 46.4, 44.8, 43.4, 39.8, 38.1, 28.5, 26.3, 24.5, 24.4, 24.0; HRMS (FAB, NBA) *m/z* 762.4158 [(M + H)⁺; calcd for C₄₆H₅₅N₃O₇ 762.4118]. Anal. Calcd for C₄₆H₅₅N₃O₇: C, 72.50; H, 7.29; N, 5.52. Found: C, 72.26; H, 7.49; N, 5.17.

PhePheLeuPhe Primary Amide (–)-28. A solution of (+)-**37** (581 mg, 0.763 mmol) in THF (50 mL) was cooled to –10 to –15 °C (NaCl/ice bath) and treated with *N*-methylmorpholine (108 mg, 1.07 mmol) followed by *i*-BuOCOCl (146 mg, 1.07 mmol). After 10 min, gaseous NH₃ was bubbled through the reaction mixture for 3–4 min. The mixture was stirred 10 min further, poured into 10% aqueous NaHSO₄ (100 mL), and extracted with EtOAc (3 × 75 mL). The combined organic solutions were washed with 10% NaHSO₄ and brine (75 mL each), dried over MgSO₄, filtered, and concentrated. Flash chromatography (65% EtOAc/hexanes) furnished **28** (580.7 mg, 100% yield) as a pale yellow solid. NMR analysis at 330 K coalesced the rotameric signals observed at ambient temperature: mp 111–113 °C; $[\alpha]_D^{25}$

–147° (c 0.99, CHCl₃); ¹³C NMR (125 MHz, CDCl₃, 330 K) δ 202.0, 201.6, 175.6, 162.3, 160.9, 152.0, 139.7, 137.1, 134.6, 130.0, 129.8, 128.9, 128.5, 128.2, 127.7, 127.0, 126.7, 126.1, 111.1, 109.6, 94.5, 80.2, 74.9, 70.2, 68.3, 64.0, 46.8, 43.8, 43.5, 39.9, 37.0, 28.5, 28.0, 26.9, 26.3, 24.5, 24.2, 23.9; HRMS (FAB, NBA) *m/z* 761.4245 [(M + H)⁺; calcd for C₄₆H₅₇N₄O₆ 761.4278]. Anal. Calcd for C₄₆H₅₆N₄O₆: C, 72.59; H, 7.43; N, 7.36. Found: C, 72.37; H, 7.64; N, 7.09.

Amino Alcohol (–)-31. The Boc acetonide (–)-**28** (508 mg, 0.668 mmol) was dissolved in anhydrous methanolic HCl (1 N, 40 mL), prepared by addition of AcCl (3.56 mL, 3.93 g, 50.0 mmol) to anhydrous methanol (46.5 mL). The mixture was stirred at room temperature until TLC analysis of an aliquot indicated that the reaction was complete (1.5 h). Prolonged reaction times led to formation of the unwanted C-terminal methyl ester. The mixture was diluted with CH₂Cl₂ (50 mL), and solid NaHCO₃ was added until fizzing from neutralization of HCl subsided. The resultant mixture was filtered through Celite, and the filter cake was rinsed with methanol and CH₂Cl₂. Concentration and flash chromatography (6% MeOH saturated with NH₃/CH₂Cl₂) gave (–)-**31** (347.0 mg, 84% yield) as a pale yellow solid: mp 106–108 °C; $[\alpha]_D^{25} -195^\circ$ (c 1.02, CHCl₃); ¹³C NMR (125 MHz, CDCl₃) δ 203.0, 201.6, 175.8, 162.5, 161.4, 139.5, 138.3, 134.7, 129.9, 129.2, 128.9, 128.7, 128.2, 127.6, 127.0, 126.6, 126.2, 110.2, 109.0, 70.9, 69.8, 68.4, 57.2, 46.1, 43.9, 43.5, 40.4, 40.2, 37.0, 24.6, 24.5, 24.0; HRMS (FAB, NBA) *m/z* 621.3457 [(M + H)⁺; calcd for C₃₈H₄₅N₄O₄ 621.3441]. Anal. Calcd for C₃₈H₄₄N₄O₄: C, 73.51; H, 7.16; N, 9.03. Found: C, 73.17; H, 7.41; N, 8.82.

Boc Primary Amide Inhibitor (–)-3. A solution of primary amine (–)-**31** (50 mg, 0.081 mmol) in CH₂Cl₂ (1 mL) was treated with Et₃N (16.3 mg, 0.161 mmol) followed by (Boc)₂O (19.3 mg, 0.0886 mmol) and stirred at room temperature for 3.5 h. The mixture was diluted with EtOAc (25 mL) and washed with 10% aqueous NaHSO₄ (20 mL), and the aqueous phase was extracted with EtOAc (25 mL). The combined organic solutions were then washed with 10% NaHSO₄ (2 × 20 mL), saturated aqueous NaHCO₃, and brine (20 mL each), dried over MgSO₄, filtered, and concentrated. Flash chromatography (90% EtOAc/hexanes) furnished **3** (44 mg, 76% yield) as a pale yellow solid: mp 122–124 °C (dec); $[\alpha]_D^{25} -168^\circ$ (c 1.0, CHCl₃); ¹³C NMR (125 MHz, CDCl₃) δ 204.0, 201.6, 175.7, 162.6, 161.0, 156.3, 139.4, 138.3, 134.2, 129.8, 129.4, 128.9, 128.5, 128.2, 127.8, 127.1, 126.5, 126.2, 109.3, 109.0, 79.5, 70.8, 68.1, 67.6, 57.2, 46.4, 43.8, 41.6, 39.2, 38.7, 37.0, 28.4, 24.51, 24.48, 24.0; HRMS (FAB, NBA) *m/z* 721.3937 [(M + H)⁺; calcd for C₄₃H₅₃N₄O₆ 721.3965].

Tetrahydrofuranyl Primary Amide Inhibitor (–)-33. A solution of primary amine (–)-**31** (357 mg, 0.575 mmol) in CH₂Cl₂ (15 mL) was treated with Et₃N (175 mg, 1.73 mmol) and (–)-**3(S)-32**³² (170 mg, 0.742 mmol) and stirred at room temperature for 2.25 h. The mixture was then diluted with CH₂Cl₂ (50 mL) and washed with 10% aqueous NaHSO₄ (2 × 30 mL). The combined aqueous phases were extracted with CH₂Cl₂ (50 mL), and the combined organic solutions were washed with saturated aqueous NaHCO₃ and brine (40 mL each), dried over MgSO₄, filtered, and concentrated. Flash chromatography (2% HOAc, 3% MeOH/EtOAc) furnished **33** (357 mg, 85% yield) as a white foam. NMR analysis at 330 K coalesced the rotameric signals observed at ambient temperature: $[\alpha]_D^{25} -216^\circ$ (c 1.0, CHCl₃); ¹³C NMR (125 MHz, CD₃OD, 330 K) δ 204.2, 202.1, 178.7, 164.8, 163.3, 158.2, 140.9, 140.1, 136.2, 131.1, 130.4, 130.1, 129.3, 129.2, 128.7, 127.9, 127.3, 127.1, 110.3, 109.8, 76.5, 74.2, 72.4, 69.7, 69.5, 67.9, 59.4, 45.5, 44.1, 43.5, 41.2, 39.7, 38.6, 33.7, 25.4, 24.9, 24.5; HRMS (FAB, NBA) *m/z* 735.3733 [(M + H)⁺; calcd for C₄₃H₅₁N₄O₇ 735.3758].

Amino Alcohol (–)-34. A solution of Boc acetonide (–)-**28** (69.0 mg, 0.0907 mmol) in methanolic HCl (1 N, 3 mL, prepared as described above) was stirred at room temperature for 18 h. Excess solid NaHCO₃ was added slowly to neutralize the HCl, and the resultant suspension was stirred for 15 min and then concentrated. The residue was partitioned between EtOAc and H₂O (15 mL each), and the aqueous phase was extracted with EtOAc (2 × 10 mL). The combined organic solutions were washed with H₂O and brine (15 mL each), dried over MgSO₄, filtered, and concentrated. Flash chromatography (6% MeOH saturated with NH₃/CH₂Cl₂) afforded **34** (34.8 mg, 61% yield) as a white foam: $[\alpha]_D^{26} -179^\circ$ (c 1.0, CHCl₃); ¹³C NMR (125 MHz, CDCl₃) δ 203.3, 200.6, 174.3, 161.6, 161.4, 138.8, 138.4, 134.9, 130.0, 129.2,

129.0, 128.6, 128.2, 127.7, 126.9, 126.5, 126.3, 110.6, 109.3, 70.8, 69.6, 67.6, 57.2, 51.7, 46.0, 43.3, 40.8, 40.5, 40.2, 38.8, 24.6, 24.4, 23.6; HRMS (FAB, NBA) m/z 658.3276 [(M + Na)⁺; calcd for C₃₉H₄₅N₃O₅Na 658.3257].

Boc Methyl Ester Inhibitor (–)-35. Primary amine (–)-34 (55 mg, 0.087 mmol) was dissolved in CH₂Cl₂ (1.1 mL) and treated with (Boc)₂O (21 mg, 0.095 mmol) and Et₃N (17.5 mg, 0.173 mmol). The reaction mixture was stirred at room temperature for 2.75 h and then partitioned between EtOAc and 10% aqueous NaHSO₄ (10 mL each). The aqueous layer was extracted with EtOAc (10 mL), and the combined organic solutions were washed with 10% aqueous NaHSO₄, saturated aqueous NaHCO₃, and brine (10 mL each), dried over MgSO₄, filtered, and concentrated. Flash chromatography (5% MeOH/CH₂Cl₂) gave **35** (35.2 mg, 65% yield) as a white foam. NMR analysis at 330 K coalesced the rotameric signals observed at ambient temperature: [α]_D²⁵ –152° (c 1.0, CHCl₃); ¹³C NMR (125 MHz, CDCl₃, 330 K) δ 204.5, 200.7, 174.2, 161.4, 161.2, 156.3, 139.1, 138.5, 134.7, 130.0, 129.5, 129.1, 128.6, 128.21, 128.15, 127.2, 126.5, 126.3, 110.8, 109.7, 79.6, 70.7, 67.9, 67.4, 57.5, 51.6, 46.7, 41.0, 41.0, 39.6, 38.8, 28.4, 24.6, 24.5, 23.8; HRMS (FAB, NBA) m/z 772.3558 [(M + Na)⁺; calcd for C₄₄H₅₃N₃O₇Na 772.3574].

Tetrahydrofuranyl Methyl Ester Inhibitor (–)-36. A solution of primary amine (–)-34 (77 mg, 0.121 mmol) in CH₂Cl₂ (3.2 mL) was treated with Et₃N (36.7 mg, 0.363 mmol) and (–)-(3S)-32³² (27.7 mg, 0.121 mmol). The reaction mixture was stirred at room temperature for 3 h and then partitioned between EtOAc and 10% aqueous NaHSO₄ (20 mL each). The aqueous phase was next extracted with EtOAc (20 mL), and the combined organic solutions were washed with 10% aqueous NaHSO₄ and brine (20 mL each), dried over MgSO₄, filtered, and concentrated. Flash chromatography afforded **36** (56.3 mg, 62% yield) as a white foam. NMR analysis at 320 K coalesced the rotameric signals observed at ambient temperature: [α]_D²⁶ –171° (c 1.0, CHCl₃); ¹³C NMR (125 MHz, CDCl₃, 330 K) δ 204.2, 200.6, 174.1, 161.9 (br), 161.4 (br), 156.3, 138.9, 138.2, 134.6, 129.9, 129.4, 129.0, 128.5, 128.2, 128.0, 127.1, 126.6, 126.3, 110.2, 109.4, 75.4, 73.2, 70.8, 67.7, 66.9, 57.9, 51.6, 46.5, 42.0, 41.1, 39.7, 38.9, 38.7, 32.8, 24.5, 24.4, 23.8; HRMS (FAB, NBA) m/z 772.3558 [(M + Na)⁺; calcd for C₄₄H₅₃N₃O₈Na 772.3574].

Hydroxy Amino *tert*-Butyl Amide (–)-38. A solution of acetonide carboxylic acid (+)-37 (57.0 mg, 0.0748 mmol) in THF (4.5 mL) was cooled to –10 °C, treated with *i*-BuOCOCl (14.3 mg, 0.105 mmol) and Et₃N (10.6 mg, 0.105 mmol), and stirred for 0.5 h. *t*-BuNH₂ (27.4 mg, 0.374 mmol) was then added, and the resultant mixture was stirred 0.5 h further, poured into 10% aqueous NaHSO₄ (10 mL), and extracted with EtOAc (2 × 15 mL). The combined organic solutions were washed with 10% NaHSO₄ (10 mL), saturated aqueous NaHCO₃ (2 × 10 mL), and brine (10 mL), dried over MgSO₄, filtered, and concentrated. Flash chromatography (35% EtOAc/hexanes) provided the *tert*-butyl amide (49.8 mg, 81% yield) as a white foam.

A solution of the acetonide *tert*-butyl amide (56 mg, 0.066 mmol) in methanolic HCl (1 N, 4.5 mL, prepared as described above) was stirred at room temperature for 18 h. Solid NaHCO₃ was added until bubbling subsided, the reaction mixture was then filtered through Celite, and the filter cake was washed with MeOH (25 mL). Following concentration under reduced pressure, the residue was partitioned between EtOAc (15 mL) and H₂O (10 mL), the aqueous phase was extracted with EtOAc (15 mL), and the combined organic solutions were washed with brine (10 mL), dried over MgSO₄, filtered, and concentrated. Flash chromatography (6% MeOH saturated with NH₃/CH₂Cl₂) furnished **38** (36.3 mg, 78% yield) as a pale yellow glass: [α]_D²⁶ –175° (c 0.99, CHCl₃); ¹³C NMR (125 MHz, CDCl₃) δ 203.3, 201.4, 172.1, 162.0, 161.2, 139.8, 138.4, 134.8, 129.9, 129.2, 129.0, 128.6, 128.1, 127.8, 127.0, 126.6, 126.0, 110.9, 110.5, 70.7, 69.7, 67.8, 57.1, 50.8, 46.0, 44.0, 43.4, 40.8, 40.1, 37.7, 28.6, 24.6, 24.4, 24.0;

HRMS (FAB, NBA) m/z 699.3872 [(M + Na)⁺; calcd for C₄₂H₅₂N₄O₄Na 699.3887].

Boc *tert*-Butyl Amide Inhibitor (–)-39. A solution of primary amine (–)-38 (22.3 mg, 0.0329 mmol) in CH₂Cl₂ (1 mL) was treated with (Boc)₂O (8.6 mg, 0.040 mmol) and Et₃N (8.3 mg, 0.082 mmol) and stirred at room temperature for 2 h. The reaction mixture was then partitioned between EtOAc (20 mL) and 10% aqueous NaHSO₄ (10 mL), and the combined organic solutions were washed with 10% aqueous NaHSO₄, saturated aqueous NaHCO₃, and brine (10 mL each), dried over MgSO₄, filtered, and concentrated. Flash chromatography (4% MeOH/CH₂Cl₂) furnished **39** (19.9 mg, 78% yield) as a white glass. NMR analysis at 330 K coalesced the rotameric signals observed at ambient temperature: [α]_D²⁵ –179° (c 0.67, CHCl₃); ¹³C NMR (125 MHz, CDCl₃, 330 K) δ 204.4, 201.6, 172.1, 161.9, 160.8, 156.3, 140.0, 138.5, 134.5, 129.9, 129.5, 129.1, 128.6, 128.18, 128.16, 127.3, 126.6, 126.1, 110.9, 79.6, 70.6, 67.9, 67.7, 56.8 (br), 50.9, 46.6, 44.3, 41.9, 39.6, 38.8, 37.8, 28.7, 28.4, 24.7, 24.5, 24.1; HRMS (FAB, NBA) m/z 799.4432 [(M + Na)⁺; calcd for C₄₇H₆₀N₄O₆Na 799.4411].

Tetrahydrofuranyl *tert*-Butyl Amide Inhibitor (–)-40. A solution of primary amine (–)-38 (18.3 mg, 0.027 mmol) in CH₂Cl₂ (1 mL) was treated with (–)-(3S)-32³² (6.2 mg, 0.027 mmol) and Et₃N (8.2 mg, 0.081 mmol) and stirred at room temperature for 2.5 h. The reaction mixture was then partitioned between EtOAc and 10% aqueous NaHSO₄ (20 mL each), the aqueous phase was extracted with EtOAc (20 mL), and the combined organic solutions were washed with 10% aqueous NaHSO₄, saturated aqueous NaHCO₃, and brine (20 mL each), dried over MgSO₄, filtered, and concentrated. Flash chromatography (5% MeOH/CH₂Cl₂) gave **40** (14.7 mg, 66% yield) as a white foam. NMR analysis at 330 K coalesced the rotameric signals observed at ambient temperature: [α]_D²⁵ –181° (c 0.97, CHCl₃); ¹³C NMR (125 MHz, CDCl₃, 330 K) δ 204.5, 201.5, 172.1, 162.0, 160.8, 156.2, 139.9, 138.2, 134.4, 129.9, 129.4, 129.1, 128.6, 128.2, 128.2, 127.4, 126.7, 126.1, 111.0, 110.9, 75.5, 73.3, 70.6, 67.7, 66.9, 57.9, 50.9, 46.5, 44.1, 41.8, 39.5, 38.5, 37.8, 32.9, 28.7, 24.6, 24.4, 24.1; HRMS (FAB, NBA) m/z 813.4215 [(M + Na)⁺; calcd for C₄₇H₅₈N₄O₇Na 813.4204].

Acknowledgment. The University of Pennsylvania authors are pleased to acknowledge support of this investigation by the National Institutes of Health (Institute of General Medical Sciences) through Grant GM-41821, Bachem, Inc. (Torrance, CA), and Merck Research Laboratories (West Point, PA). We also thank Drs. G. Furst, P. Carroll, and Mr. J. Dykins, Directors of the University of Pennsylvania Spectroscopic Facilities, for assistance in obtaining NMR spectra, X-ray crystal structures, and high-resolution mass spectra, respectively. A.P. thanks the American Cancer Society for a postdoctoral fellowship.

Supporting Information Available: Stereoview of the docking of peptidomimetic **4** in the HIV-1 protease active site, table of the various Lewis acid conditions employed in the alkylation with epoxide studies, and text describing complete spectroscopic and analytical data for **3–5**, **7**, **11–13**, **16**, **17**, **19**, **21**, **23–28**, **31**, **33–40**, and several characterized intermediates as well as experimental procedures for the Lewis acid mediated alkylations (18 pages). This material is contained in many libraries on microfiche, immediately follows this article in the microfilm version of the journal, can be ordered from the ACS, and can be downloaded from the Internet; see any current masthead page for ordering information and Internet access instructions.

JA951371W